Supporting Information

Functional hBN decorated $Ni(OH)_2$ nanosheet synthesized for remarkable adsorption performance for the elimination of fluoride ions.

Diksha Choudhary[1,2], Ankit Singh[1], Abhishek Giri[1], Harish Chandra Prasad[1,2], R.K. Sharma[3], Alka Mishra[1,2] Sandeep Singhai[1,2], Archana Singh[1,2] *

[1] Academy of Scientific and Innovative Research (AcSIR), Ghaziabad, 201002, India.
[2] Centre for Advanced Radiation Shielding and Geopolymeric Materials, CSIR-Advanced Materials and Processes Research Institute, Bhopal, 462026, India
[3]Technical Physical Division, Bhabha Atomic Research Center Trombay, Mumbai, 400085, India.

Powder x-ray diffraction: - The crystalline phase of the samples has been investigated via X-ray diffraction (Bruker AXS with D8 advance instrument) using Cu Kα radiation (k = 1.5406).

Williamson-Hall (W-H) method was employed to determine the influence of micro strain (ε = slope) present in prepared powder samples and information of crystallite size (intercept = $\frac{k\lambda}{Dw}$) of the samples, calculated by using the following formula:

$$\beta_{hkl}\cos\theta = \frac{k\lambda}{Dw} + 4\varepsilon \sin\theta \quad \text{.....(1)}$$

Where λ is the X-ray wavelength (1.5405 Å), 0.89 is shape constant, ε is the induced strain in the crystal, and β is FWHM in radians. A graph is plotted between β cosθ and 4 sinθ, and the linear fitting of graph intercept and slope of the line is used to compute the average crystallite size and micro strain [1]. Table 2 summarizes these results.

Dislocation density (δ) represents the number of defects present in a system and is defined as the length of dislocation lines per unit volume in the crystal, calculated by using the following formula:

$$\delta = \frac{1}{D^2} \quad \text{.....(2)}$$

Where D is the crystallite size in nm.

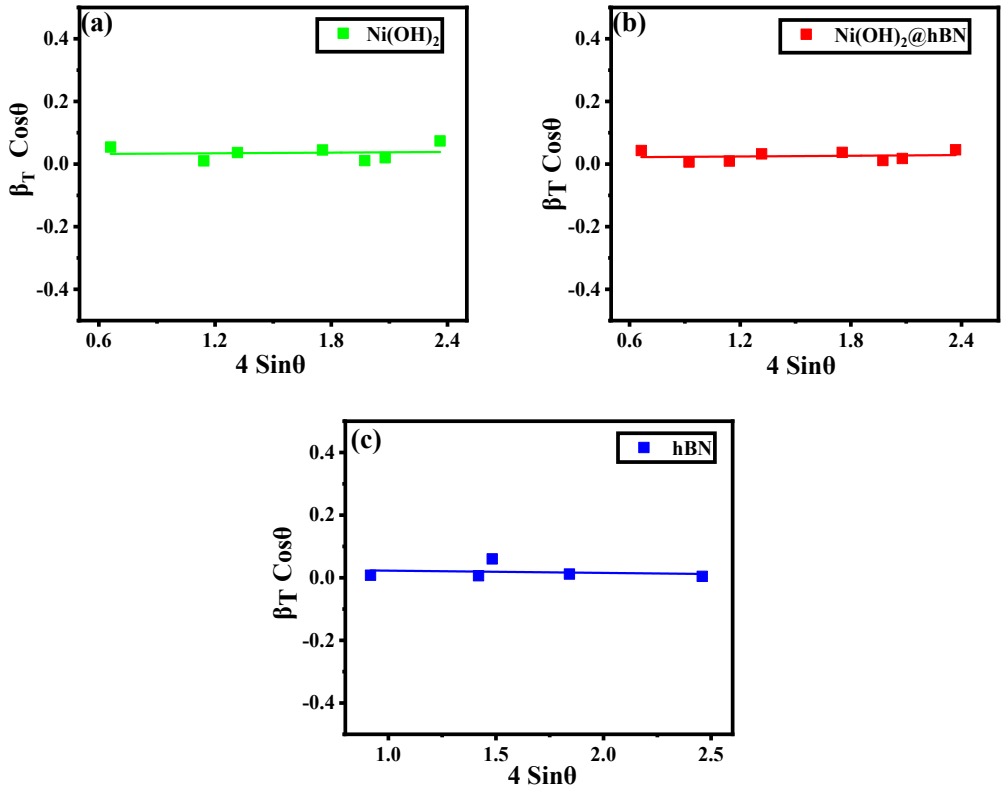

Figure S1 W-H plot of $Ni(OH)_2$ (a), and $Ni(OH)_2$@hBN (b), and hBN (c).

Table S1 Illustration of lattice parameters, cell volume, and crystallite size using W-H plot, strain, and dislocation density of all three material.

Sample Name	Lattice Parameter a(Å)	c(Å)	Volume (Å)^3	Crystallite Size D (nm)	Strain ε (10^{-4})	Dislocation Density δ (10^{-3})
$Ni(OH)_2$	3.126	4.605	38.97	4.6218	0.00359	0.04681
$Ni(OH)_2$ @hBN	3.126 2.504	4.605 6.661	38.97 36.17	7.0814	0.0038	0.01994
hBN	2.504	6.661	36.17	4.64813	-0.00718	0.04628

A graph is plotted between β cosθ and 4 sinθ, and the linear fitting of graph intercept and slope of the line is used to compute the average crystallite size and microstrain (Figure S1) [2]. Table S1 summarizes these results. The positive slope of the graph is attributed to the presence of minor strain in $Ni(OH)_2$@hBN, which can be caused during the synthesis process. This behavior could be attributed to the synergistic relationship between $Ni(OH)_2$ and hBN to form the specific structure of the adsorbent, which is favorable for fluoride adsorption. From Table S1, it can be observed that dislocation density decreases in $Ni(OH)_2$@hBN, which attributes to the formation of less defect and perfection in the lattice structure, compare to single $Ni(OH)_2$ and hBN.

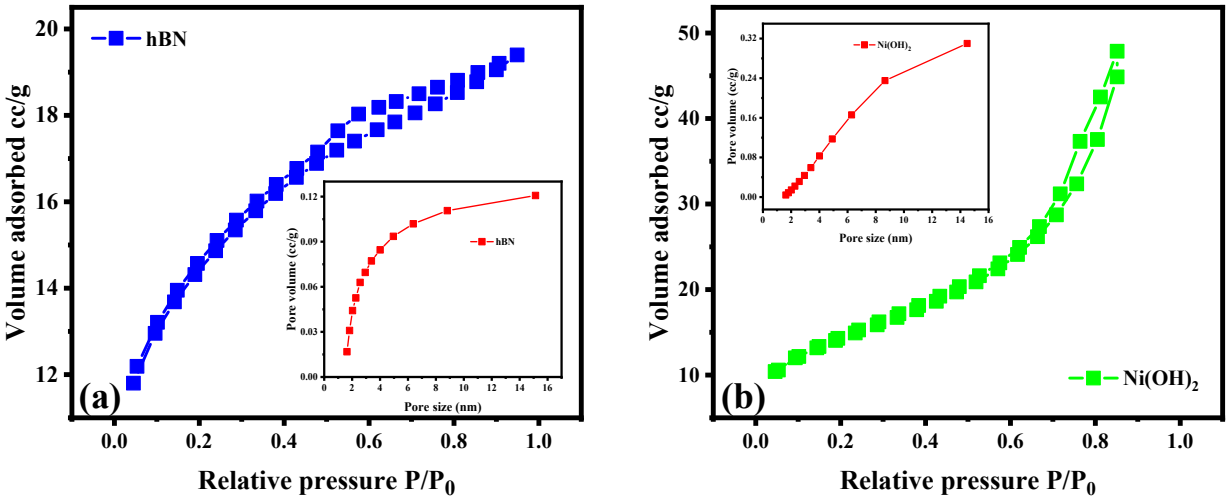

Figure S2 N_2 adsorption–desorption isotherm, and inset pore size distribution of hBN (a), and $Ni(OH)_2$ (b).

Experimental section: -In a batch experiment study, 250 ml of conical flasks is filled with 100 ml of fluoride solution (concentration 100 mg/L), and then 0.02 g of $Ni(OH)_2$@hBN was added. Fluoride stock solution concentration was confirmed by "IS 3025(Part 60): 2008 (RA 2012) Electrochemical probe method, APHA 23rd Edition 2017, 4500 Fluoride" method. After the application solution and material were separated, and the elemental concentration of water was checked by ICP-MS. A Thermo Scientific X Series II ICP-MS (Thermo Fisher Scientific, Bremen, Germany) was used for Nickel and Boron elemental detection. Below mentioned results show that there is no leaching of material into the water. Also, nickel and boron have concentrations under the permissible limit of WHO (World Health Organization file (1) WHO/SDE/WSH/03.04/96, (2) WHO/HEP/ECH/WSH/2021.6 (3) WHO/HSE/WSH/09.01/2) drinking water standards, and support good material stability.

Table S1 shows the element concentration of participating elements.

Element	Concentration	Permissible limit
Fluoride (Stock solution)	100 mg/L (approx.)	1.5 mg/L
Nickel (Ni)	0.01 mg/L (approx.)	0.02 mg/L
Boron (B)	0.03 mg/L (approx.)	2.4 mg/L

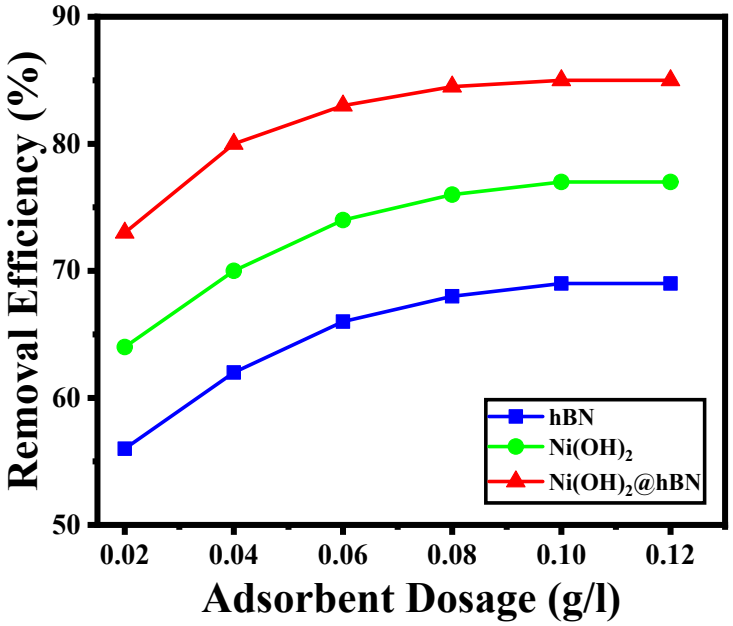

Figure S3 Effect of adsorbent dose on fluoride removal efficiency %.

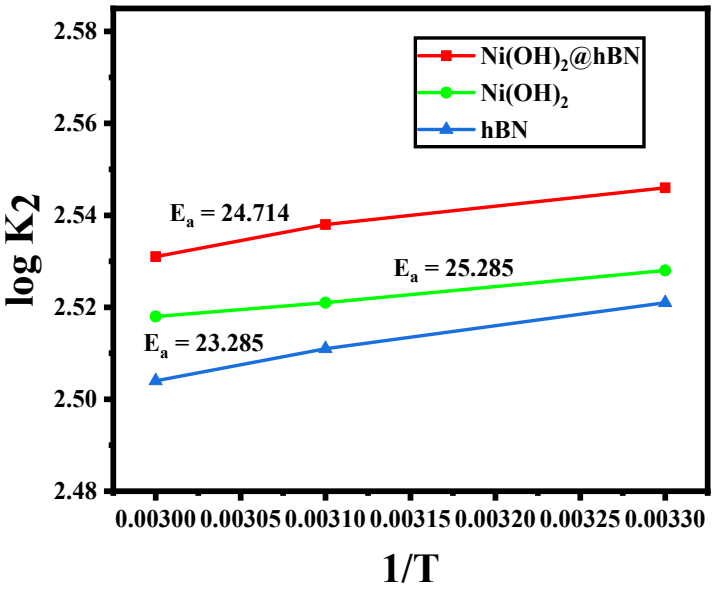

Figure S4 Activation energy plot for fluoride adsorption by $Ni(OH)_2$@hBN, hBN and $Ni(OH)_2$.

Regeneration treatment of $Ni(OH)_2$@hBN: -

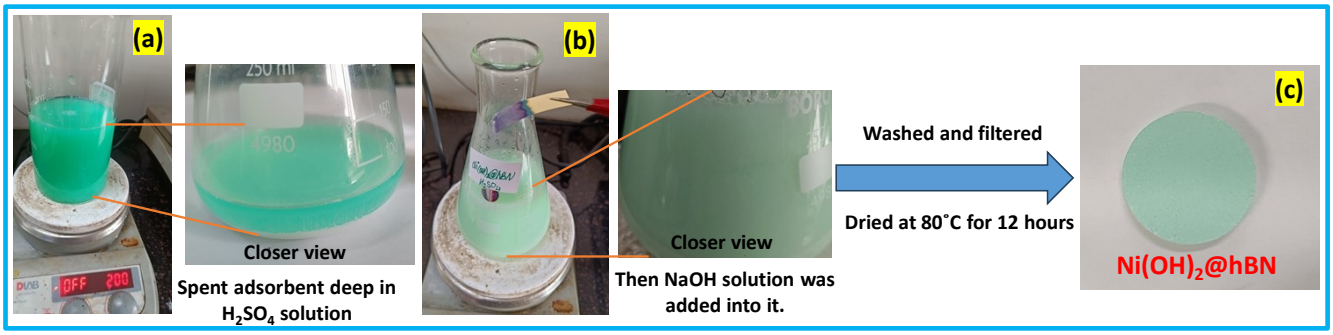

Scheme S1 Showing the chemical reaction of regeneration method.

To further confirmed the composition of regenerated $Ni(OH)_2$@hBN, X-ray fluorescence spectroscopy (XRF) analysis was used.

XRF Analysis: - The Bruker India Scientific XRF Model S8 Tiger, and powder samples with 40 mm diameter pallet are used to better understand the chemical composition of materials before and after recycling. A comparison of raw and recycled $Ni(OH)_2$@hBN materials concentration is mentioned in the table. Its results suggested that nickel is bonded with oxygen, hence its regeneration is a successful method.

Table S2. XRF result of raw and recycled $Ni(OH)_2$@hBN

S no.	Main constituent	Raw Sample (wt %)	Recycled Sample (wt %)
1.	Ni-O	90.8 %	91.3 %
2.	B-N	9.2 %	8.7 %

This recycled material only reduces 7% fluoride removal efficiency after 1st cycle. The current results prove that the material has great potential for practical application as a relatively smaller amount of reagents and raw materials were utilized to synthesize $Ni(OH)_2$@hBN.

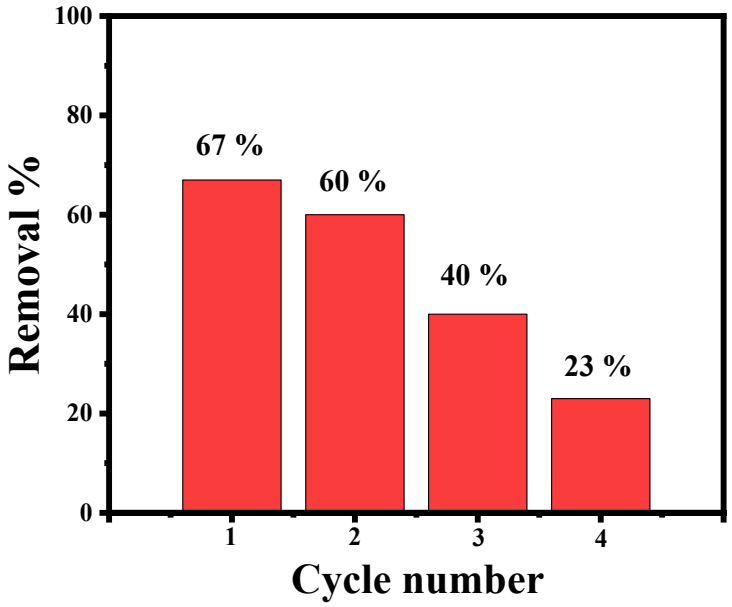

Figure S5 Variation of the removal rates of fluoride onto $Ni(OH)_2$@hBN in successive cycles.

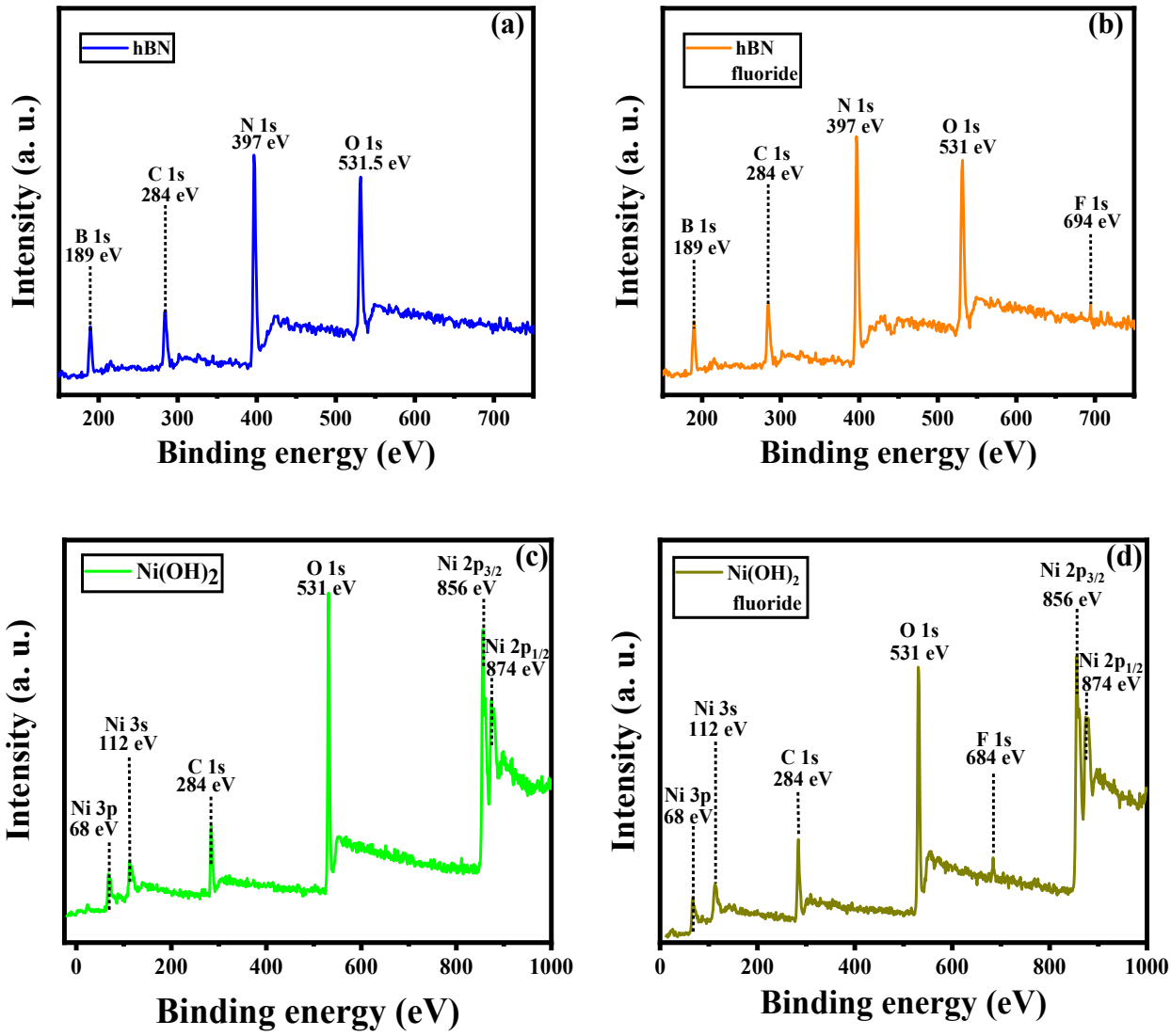

Figure S6 XPS survey spectra of hBN, and $Ni(OH)_2$, (a,c,) before adsorption, and after fluoride adsorption (b,d,) on hBN, and $Ni(OH)_2$, surface.

Reference

1. Bhardwaj, P., et al., *Structural, optical and magnetic characterization of Ni2+ ions doped chromium oxide (Cr2O3) nanoparticles.* Solid State Sciences, 2021. **115**: p. 106581.

2. Desai, K.R., et al., *X-ray diffraction based Williamson–Hall analysis and rietveld refinement for strain mechanism in Mg–Mn co-substituted CdFe2O4 nanoparticles.* Physica B: Condensed Matter, 2021. **614**: p. 413054.